

Nonextensive Supercluster States in Aggregation with Fragmentation

 Nikolai V. Brilliantov^{1,2}, Wendy Otieno,² and P. L. Krapivsky^{1,3,4}
¹*Skolkovo Institute of Science and Technology, 143026 Moscow, Russia*
²*Department of Mathematics, University of Leicester, Leicester LE1 7RH, United Kingdom*
³*Department of Physics, Boston University, Boston, Massachusetts 02215, USA*
⁴*Santa Fe Institute, 1399 Hyde Park Road, Santa Fe, New Mexico 87501, USA*
 (Received 17 January 2021; revised 13 October 2021; accepted 27 October 2021; published 17 December 2021)

Systems evolving through aggregation and fragmentation may possess an intriguing supercluster state (SCS). Clusters constituting this state are mostly very large, so the SCS resembles a gelling state, but the formation of the SCS is controlled by fluctuations and in this aspect, it is similar to a critical state. The SCS is nonextensive, that is, the number of clusters varies sublinearly with the system size. In the parameter space, the SCS separates equilibrium and jamming (extensive) states. The conventional methods, such as, e.g., the van Kampen expansion, fail to describe the SCS. To characterize the SCS we propose a scaling approach with a set of critical exponents. Our theoretical findings are in good agreement with numerical results.

 DOI: [10.1103/PhysRevLett.127.250602](https://doi.org/10.1103/PhysRevLett.127.250602)

Aggregation processes [1–3] are ubiquitous in nature, social life, and technology [4–7]. For instance, they underlie self-assembly, where preexisting elemental entities bind together due to local interactions [8,9]. Aggregation processes take place at diverse temporal and spatial scales ranging from molecular scales [10–12] and macroscopic scales where they influence clouds and rain [13–16] to astrophysical scales where, e.g., aggregation of cosmic dust grains drives planetesimal and planetary ring formation [17–23]. Technological objects like swarm-bots also demonstrate aggregation and self-assembling [24]. In social networks, the merging units may be internet users, enterprises, etc. [7,25,26].

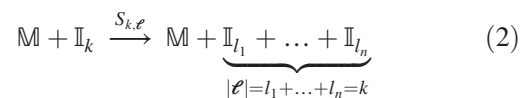
In addition processes, the merging occurs only by addition of elemental units. Symbolically (see Fig. 1),



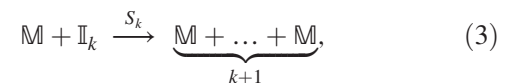
Here, $\mathbb{M} \equiv \mathbb{I}_1$ denotes an elementary entity, a monomer, \mathbb{I}_k is a cluster comprised of k units, and A_k is the rate of the process. Addition processes underlie self-assembly [9–12,27], internet, and business systems. In materials science, the addition mechanism dominates when the mobility of monomers greatly exceeds the mobility of larger clusters [28–30]. This happens in several surface processes when adatoms (monomers) diffuse on a substrate [28–37], synthesis of nanocrystals [38,39], aggregation of point defects in solids [40,41], etc. The Becker-Döring equation [42–46] and the Lifshitz-Slyozov-Wagner model also rely [47,48] on the addition mechanism.

Aggregation is often accompanied by cluster disintegration that may occur, e.g., due to the accumulation of faulty steps in self-assembling. Disintegration can proceed spontaneously [42–47] or be caused by interactions with

monomers that trigger either addition or disintegration. The reaction scheme



represents the breakage into the debris $\ell = \{l_1, \dots, l_n\}$. The collision-controlled fragmentation underlies, e.g., the Oort-Hulst models [49–53]. Generally, the process (2) describes the breakup of an aggregate in a collision with energetic monomers [21,54–57]. The complete breakage,



is known as the shattering process [5,19,21,58]; it is included in the Oort-Hulst models. Qualitatively similar behaviors emerge for partial (2) and complete (3) breakage, provided that a large number of elementary units is produced. Here we present the analysis for the shattering

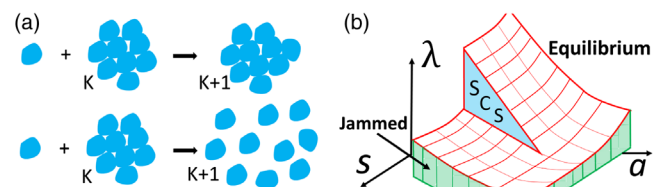


FIG. 1. (a) Additional aggregation with disintegration. (b) Schematic phase diagram of aggregating systems with disintegration in the (a, s, λ) domain. The nonextensive SCS lie on a surface that is surrounded by the extensive jammed states and equilibrium steady states.

model (3); the results for the general model (2) are given in the Supplemental Material [59].

Here we investigate addition-shattering processes and observe rich behaviors. Besides the equilibrium states (ESs) and jammed states (JSs), we reveal intriguing super-cluster states (SCSs) composed of mostly very large clusters. The SCSs are nonextensive—the number of emerging structures does not scale linearly with the system size; furthermore, fluctuations play a dominant role there. Conventional approaches fail to describe the SCS and we propose a framework to characterize it. Below detailed definitions of JSs and SCSs are given.

Addition and shattering rates often vary algebraically with the aggregate size. We thus consider the rates

$$A_k = k^a, \quad S_k = \lambda k^s. \quad (4)$$

The amplitude in addition rate is set to unity by time rescaling. The dependence (4) with $a \leq 1$ simply reflects the fact that the aggregation rate is proportional to the clusters surface (which may be fractal); the aggregation in networks also obeys (4) with $a \leq 1$ [7,60]. The intensity of the shattering process is quantified by λ , while the exponent s depends on its mechanism; commonly $s \leq 1$.

Denote by $c_k(t)$ the density of aggregates of size k . With rates (4), the governing equations read

$$\frac{dc_1}{dt} = -c_1^2 - \sum_{j=1}^{\infty} j^a c_1 c_j + \lambda \sum_{j=2}^{\infty} j \cdot j^s c_1 c_j, \quad (5a)$$

$$\frac{dc_k}{dt} = c_1 [(k-1)^a c_{k-1} - k^a c_k] - \lambda k^s c_1 c_k. \quad (5b)$$

Equation (5b) is valid for all $k \geq 2$. The right-hand side of Eq. (5a) reflects that the monomer density decreases due to aggregation with other monomers and clusters (first and second terms) and increases due to shattering.

First, we illustrate the generic behavior of the system on tractable models. Then a conjecture about its general behavior is confirmed numerically.

Model with $(a, s) = (1, 0)$.—In terms of the modified time, $\tau = \int_0^t c_1(t') dt'$, Eqs. (5a) and (5b) linearize

$$\dot{c}_1 = -(1 + \lambda)c_1 - 1 + \lambda, \quad (6a)$$

$$\dot{c}_k = (k-1)c_{k-1} - (k+\lambda)c_k, \quad k \geq 2. \quad (6b)$$

Hereinafter $\dot{f} \equiv df/d\tau$. We choose the units where the mass density conservation reads $M_1 = \sum_{k \geq 1} k c_k = 1$. Solving (6a) for the most natural monodisperse initial conditions, $c_k(0) = \delta_{k,1}$, we obtain

$$c_1(\tau) = \frac{2}{1 + \lambda} e^{-(1+\lambda)\tau} - \frac{1 - \lambda}{1 + \lambda}. \quad (7)$$

This exact result shows that different behaviors emerge depending on whether λ is less than, equal to, or larger than $\lambda_c = 1$: If $\lambda \geq \lambda_c = 1$, the monomer density $c_1(\tau)$ always remains non-negative, while for $\lambda < 1$, the monomer density formally becomes negative as a function of the modified time. The requirement $c_1 \geq 0$ implies the existence of τ_{\max} such that the system evolves only until $\tau \leq \tau_{\max}$, where $c_1(\tau_{\max}) = 0$; the modified time τ_{\max} corresponds to the infinite physical time $t = \infty$, see Supplemental Material [59].

In the subcritical case, $\lambda < 1$, the relation between t and τ is found from Eq. (7) yielding

$$c_1(t) = \frac{1 - \lambda}{2e^{(1-\lambda)t} - 1 - \lambda}.$$

Thus the monomer density vanishes at $t \rightarrow \infty$ if $\lambda < 1$. Other cluster densities remain positive. Near the critical point ($0 < 1 - \lambda \ll 1$), they simplify to (see Supplemental Material [59])

$$c_k(\infty) = \left[\frac{1}{2} - \frac{1}{k(k+1)} \right] (1 - \lambda) + O[(1 - \lambda)^{3/2}]. \quad (8)$$

Final densities depend on the initial condition, see Fig. 2. Hence, for $\lambda < 1$ the system falls into a jammed state—a nonequilibrium stationary state, with a structure depending on initial conditions, e.g., Refs. [61,62]. Additionally, in our systems monomers vanish in the JSs (see Supplemental Material [59]).

At the critical point $c_k = e^{-2\tau}(1 - e^{-\tau})^{k-1}$ if $c_k(0) = \delta_{k,1}$. From $c_1(\tau) = e^{-2\tau}$, we get $2\tau = \ln(1 + 2t)$ and

$$c_k = \frac{1}{1 + 2t} \left[1 - \frac{1}{\sqrt{1 + 2t}} \right]^{k-1}, \quad c = \frac{1}{\sqrt{1 + 2t}}, \quad (9)$$

where $c = \sum_{k \geq 1} c_k$ is the total cluster density. All densities vanish at $t = \infty$ independently on initial conditions, yet the

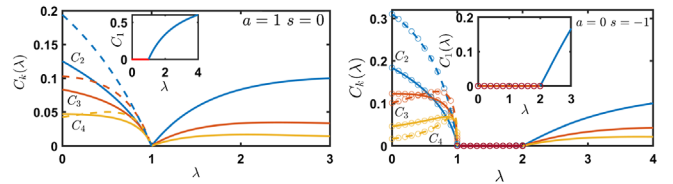


FIG. 2. Left panel: The final densities $c_k(\lambda) \equiv c_k(t = \infty)$ versus λ for the model $(a, s) = (1, 0)$. Initial conditions are monodisperse (solid lines); monomer-dimer, specifically $c_1(0) = 0.2$ and $c_2(0) = 0.4$, (dashed lines). Right panel: The same for the model $(a, s) = (0, -1)$. Curves: analytical (for $\lambda \geq 1$) and numerical (for $\lambda < 1$) solutions of rate equations; dots: Monte Carlo (MC) results. The system size is $N = 10^6$. All densities vanish in the SCS at $\lambda = 1$ (left panel) and $1 \leq \lambda \leq 2$ (right panel). Insets: The final density of monomers $c_1(\lambda)$.

mass density is conserved, $M_1 = 1$. The same is true for pure aggregation, where a single cluster (gel) is eventually formed in a finite-size system. As we show below, the ultimate state for a finite size system dramatically differs here: The final number of clusters varies from realization to realization and its average scales sublinearly with the system size. We call such states supercluster states (SCSs), providing a precise definition below. The SCSs manifest themselves by the vanishing densities $c_k(\infty)$ for all k in the thermodynamic limit.

In the supercritical regime $\lambda > 1$, the cluster densities relax exponentially fast to the equilibrium steady state that does not depend on initial conditions, see Supplemental Material [59]:

$$c_k(\infty) = (\lambda - 1) \frac{\Gamma(k)\Gamma(1 + \lambda)}{\Gamma(k + 1 + \lambda)}. \quad (10)$$

Equations (8)–(10) demonstrate that $c_k(\infty) \rightarrow 0$ when $\lambda \rightarrow 1 \pm 0$, indicating that at $\lambda = 1$ the system undergoes a continuous phase transition from the jammed state to the equilibrium steady state through the critical SCS with vanishing densities, see Fig. 2.

Model with $(a, s) = (0, -1)$.—The rate equations read

$$\dot{c}_1 = -(1 + \lambda)c_1 + (\lambda - 1)c, \quad (11a)$$

$$\dot{c}_k = c_{k-1} - (1 + \lambda/k)c_k \quad k \geq 2, \quad (11b)$$

The model with $\lambda_c = 1$ again demarcates different evolution regimes. In the subcritical regime, $\lambda < 1$, the system falls into a jammed state with vanishing monomer density, $c_1(\tau_{\max}) = 0$; the final cluster densities $c_k(\tau_{\max})$ are determined by initial conditions, see Fig. 2.

At the critical point, $\lambda = 1$, the solution for $t \gg 1$ reads (see Supplemental Material [59])

$$c_k(t) \simeq k^{k-1}(1 + 2t)^{-\frac{k+1}{2k}}, \quad (12)$$

indicating that all densities vanish at the critical point, see Fig. 2. When $\lambda > 1$, the Laplace transform of the densities is obtained iteratively from Eqs. (11) to give

$$\hat{c}_k(p) = \frac{1}{p} \frac{(1 + \lambda\epsilon)\epsilon^k}{F[2, 2; 2 + \lambda\epsilon; \epsilon]} \frac{k!\Gamma(1 + \lambda\epsilon)}{\Gamma(k + 1 + \lambda\epsilon)}, \quad (13)$$

where $\hat{c}_k(p) = \int_0^\infty c_k(\tau)e^{-p\tau}d\tau$ and $\epsilon = (1 + p)^{-1}$. The hypergeometric function appearing in Eq. (13) admits an integral representation

$$F[2, 2; 2 + \lambda\epsilon; \epsilon] = \lambda\epsilon(1 + \lambda\epsilon) \int_0^1 dx \frac{x(1-x)^{\lambda\epsilon-1}}{(1-x\epsilon)^2}. \quad (14)$$

Using Eqs. (13) and (14), one can extract the asymptotic behavior of $c_k(\tau)$ at $\tau \rightarrow \infty$, from the behavior of $\hat{c}_k(p)$ at

$p \rightarrow 0$. For $\lambda > 2$ the function F is regular at $p = 0$ and equals to $\lambda(1 + \lambda)/(\lambda - 2)$. The Laplace transform $\hat{c}_k(p)$ has a simple pole, $\hat{c}_k(p) \rightarrow c_k(\infty)/p$ as $p \rightarrow 0$, indicating the existence of a steady state size distribution, $c_k(\infty)$.

Within the critical interval $1 \leq \lambda \leq 2$ the function $F[2, 2; 2 + \lambda\epsilon; \epsilon]$ diverges as $p \rightarrow 0$ implying $c_k \rightarrow 0$ for $\tau \rightarrow \infty$. Overall, the final densities read

$$c_k(\infty) = \begin{cases} c_k(\tau_{\max})(1 - \delta_{k,1}) & \lambda < 1 \\ 0 & 1 \leq \lambda \leq 2 \\ \frac{k!(\lambda-1)(\lambda-2)\Gamma(\lambda)}{\Gamma(k+1+\lambda)} & \lambda > 2, \end{cases} \quad (15)$$

with $c_k(\tau_{\max})$ depending on initial conditions. The system undergoes continuous phase transitions from a JS to a SCS at $\lambda = \lambda_{\text{low}} = 1$ and from a SCS to an ES at $\lambda = \lambda_{\text{up}} = 2$. The cluster densities decay algebraically when $1 < \lambda < 2$ and logarithmically when $\lambda = 2$, see Supplemental Material [59].

Models with $s = a - 1$.—The rate equations read

$$\dot{c}_1 = -(1 + \lambda)c_1 + (\lambda - 1)M_a, \quad (16a)$$

$$\dot{c}_k = (k - 1)^a c_{k-1} - k^a(1 + \lambda/k)c_k, \quad k \geq 2, \quad (16b)$$

with $M_a = \sum_{k \geq 1} k^a c_k$. The SCS occurs (see Supplemental Material [59]) when

$$1 = \lambda_{\text{low}} \leq \lambda \leq \lambda_{\text{up}} = 2 - a \quad (17)$$

and the final densities are

$$c_k(\infty) = \begin{cases} (1 - \delta_{k,1})c_k(\tau_{\max}) & \lambda < 1 \\ 0 & 1 \leq \lambda \leq 2 - a \\ \frac{k^{-a}k!/\Gamma(k+\lambda+1)}{\sum_{n \geq 1} n^{1-a}n!/\Gamma(n+\lambda+1)} & \lambda > 2 - a. \end{cases} \quad (18)$$

Thus for the three-parameter class of models (4), the SCS [characterized by $c_k(\infty) = 0$] emerges when $s = a - 1$ and $1 \leq \lambda \leq 2 - a$, with a continuous phase transition from the SCS to the JS at $\lambda = 1$, and to the ES at $\lambda = 2 - a$. The relaxation to the JS and ES is exponentially fast, while to the SCS is algebraic in time, when $1 \leq \lambda < 2 - a$, and logarithmic for $\lambda_{\text{up}} = 2 - a$, see Supplemental Material [59].

In the Supplemental Material [59] we show that the emergence of SCSs is robust to incomplete shattering, provided that monomers are abundantly produced. For instance, it occurs if only half of a cluster disintegrates into monomers. The appearance of SCSs requires a faster growth with the cluster size of the aggregation rate than of the fragmentation rate. The latter however should be large enough to provide abundant monomers feeding the large clusters.

A detailed analysis shows that at $\lambda = \lambda_{\text{low}} = 1$, the system undergoes an infinite sequence of weak first-order phase transitions (see Supplemental Material [59]). They occur at critical values $a_1 = 1$, $a_2 = 0.415$, $a_3 = 0.224$, etc., and are manifested by an abrupt change of the relaxation kinetics of the cluster densities [63], see Supplemental Material [59].

Monomers also play a key role in Becker-Döring models with evaporation and Oort-Hulst models, yet the production of monomers never ceases in these models and hence the jammed and supercluster states do not emerge.

The nature of the SCS.—To understand the difference between SCSs and gelling states we consider large, but finite systems of $N \gg 1$ monomers. Denote by $C_k(t)$ the total number of clusters of size k and by $C(t)$ the total number of clusters. The densities $c_k(t) = C_k(t)/N$ and $c(t) = C(t)/N$ usually do not depend on the system size when $N \gg 1$. The rate Eqs. (5) describe the evolution for $c_k(t)$, but they can fail, as the usage of the densities is based on the tacit assumption that the behavior is extensive, see Supplemental Material [59]. Generally, finite stochastic systems are explored by explicitly modeling each elementary reaction. That is, in a single reaction event a configuration (C_1, C_2, \dots, C_N) transforms into one of the following:

$$(C_1 - 2, C_2 + 1) \quad \text{rate } C_1(C_1 - 1)/N, \quad (19a)$$

$$(C_1 - 1, C_k - 1, C_{k+1} + 1) \quad \text{rate } k^a C_1 C_k / N, \quad (19b)$$

$$(C_1 + k, C_k - 1) \quad \text{rate } k^s C_1 C_k / N. \quad (19c)$$

(Only the components of an evolved configuration that differ from the original configuration are shown.) The reaction rates correspond to the rates (4) and account automatically for the finiteness of the system. The quantities $C_k(t)$ are random variables and the system is characterized by the averages $\langle C_k(t) \rangle$, $\langle C_k(t) C_j(t) \rangle$, etc.

We have performed MC simulations, using the approach of Ref. [64], and observed that for $N \gg 1$ the MC results for $\langle C_k(t) \rangle$ coincide with predictions of rate equations outside the domain, associated with the SCSs, see Fig. 2(b). In the latter domain, however, the final number of clusters cannot be predicted by rate equations. We have observed a sublinear scaling: $\langle C_k(\infty) \rangle \sim N^\gamma$ and $\langle C(\infty) \rangle \sim N^\delta$ with $\gamma, \delta < 1$, see Fig. 3. The nonextensive behavior of these quantities explains the vanishing densities: $c_k(\infty) \sim N^{-(1-\gamma)}$ and $c(\infty) \sim N^{-(1-\delta)}$ in the thermodynamic limit. This enigmatic transition from extensive to the observed nonextensive behavior is caused by fluctuations. To gain analytical understanding, we employ the van Kampen expansion [5,65]

$$C_k(t) = N c_k(t) + \sqrt{N} \eta_k(t). \quad (20)$$

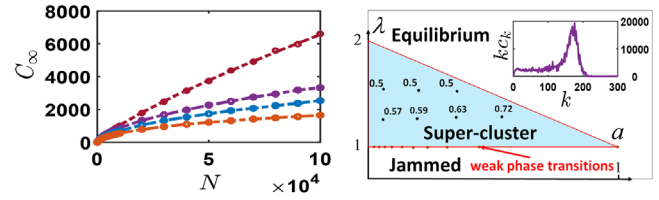


FIG. 3. Left panel: The total number of clusters in the final SCS versus N . MC results are shown by dots; fits for the scaling law, $C(\infty) \sim N^\delta$, are shown by lines. Curves (top to bottom): $(a, s, \lambda) = (1, 0, 1)$ with $\delta = 4/5$, see Eq. (29); $(a, s, \lambda) = (0, -1, 125)$ with $\delta = 0.571$; $(a, s, \lambda) = (0, -1, 135)$ with $\delta = 0.599$; $(a, s, \lambda) = (0, -1, 1.5)$ with $\delta = 0.5$. Right panel: SCS in the (a, λ) domain. It borders JSs at $\lambda_{\text{low}} = 1$ and ESSs at $\lambda_{\text{up}} = 2 - a$. The black dots with numbers indicate the values of δ . The red dots indicate the points of the weak first-order phase transitions. Inset: The mass distribution $k C_k(\infty)$ for $(a, s, \lambda) = (0, -1, 1.25)$ and $N = 10^6$.

The terms linear in N are deterministic, and the densities $c_k(t)$ obey (5). The terms proportional to \sqrt{N} are stochastic, $\eta_k(t)$ are random variables. To proceed we consider the most simple SCS at $(a, s, \lambda) = (1, 0, 1)$ for which a complete analytical solution is available. Using reaction rules (19) we deduce equations for the averages

$$N \frac{d\langle C_1 \rangle}{dt} = -2\langle C_1(C_1 - 1) \rangle, \quad (21a)$$

$$N \frac{d\langle C_2 \rangle}{dt} = \langle C_1(C_1 - 1) \rangle - 3\langle C_1 C_2 \rangle, \quad (21b)$$

$$N \frac{d\langle C_k \rangle}{dt} = (k - 1)\langle C_1 C_{k-1} \rangle - (k + 1)\langle C_1 C_k \rangle, \quad (21c)$$

with Eq. (21c) valid for $k \geq 3$. Equations (21) involve $\langle C_1 C_k \rangle$ with $k \geq 1$. The simplest such quantity, $\langle C_1^2 \rangle$, obeys

$$N \frac{d\langle C_1^2 \rangle}{dt} = 6\langle C_1^2 \rangle - 4\langle C_1 \rangle - 4\langle C_1^3 \rangle + W_1, \quad (22)$$

where $W_1 = \sum_{k \geq 1} k(k + 1)\langle C_1 C_k \rangle$. One finds $\langle \eta_k \rangle = 0$ for all k , see Supplemental Material [59]. Hence $\langle C_1 \rangle = N c_1$ and

$$\langle C_1^2 \rangle = N^2 c_1^2 + N V_1, \quad (23a)$$

$$\langle C_1^3 \rangle = N^3 c_1^3 + 3N^2 c_1 V_1 + N^{3/2} \langle \eta_1^3 \rangle, \quad (23b)$$

$$\langle C_1 C_k \rangle = N^2 c_1 c_k + N \langle \eta_1 \eta_k \rangle, \quad (23c)$$

where $V_1 = \langle \eta_1^2 \rangle = [\langle C_1^2 \rangle - \langle C_1 \rangle^2]/N$. Using Eqs. (21a) and (22) together with expansions (23), we deduce

$$\dot{V}_1 + 8V_1 = \sum_{k \geq 1} k(k + 1)c_k + 2c_1 = 2e^\tau + 2e^{-2\tau} \quad (24)$$

from which $V_1 = \frac{2}{9}e^\tau + \frac{1}{3}e^{-2\tau} - \frac{5}{9}e^{-8\tau}$, or

$$V_1 = \frac{2}{9}\sqrt{1+2t} + \frac{1}{3}(1+2t)^{-1} - \frac{5}{9}(1+2t)^{-4} \quad (25)$$

in the physical time; that is, fluctuations diverge. Hence we propose the definition of SCSs, based on this most prominent property: SCS is a state, where characteristics of a system (clusters number), associated with fluctuations, prevail over their deterministic counterparts; the characteristics scale sublinearly with the system size, leading to vanishing densities (cluster densities) in the thermodynamic limit. The total number of monomers

$$C_1(\tau) = Ne^{-2\tau} + \sqrt{N}\eta_1(\tau) \quad (26)$$

exhibits mostly deterministic decay as long as the deterministic part greatly exceeds the stochastic part. Since $V_1 = \langle \eta_1^2 \rangle \simeq \frac{2}{9}e^\tau$ for $\tau \gg 1$, the stochastic part scales as $\sqrt{N}\sqrt{V_1} \sim \sqrt{N}e^{\tau/2}$. At time τ_* , when the deterministic part becomes comparable with the stochastic part,

$$Ne^{-2\tau_*} \sim \sqrt{N}e^{\tau_*/2}, \quad (27)$$

the system enters the SCS. Using Eq. (27) and $2t = e^{2\tau} - 1$ we obtain an estimate of the time when the SCS emerges,

$$t_* \sim N^{2/5}, \quad (28)$$

supported by simulations [Fig. 4(a)]. At $t > t_*$ the system resides in the SCS where the van Kampen expansion fails.

Simulations show that after entering the SCS, the system quickly reaches the final stationary state with vanishing number of monomers, $C_1 = 0$; see Supplemental Material [59]. Thus, $\langle C_k(\infty) \rangle \simeq \langle C_k(t_*) \rangle$ for $k \geq 2$. This allows us to estimate the final cluster distribution in the SCS from the crossover time (28) and the deterministic distribution (9), written in the scaling form as $c_k \simeq (2t)^{-1}e^{-k/\sqrt{2t}}$ and $c \simeq (2t)^{-1/2}$. Using $\langle C_k \rangle \sim Nc_k$ and $t \sim t_*$ we find

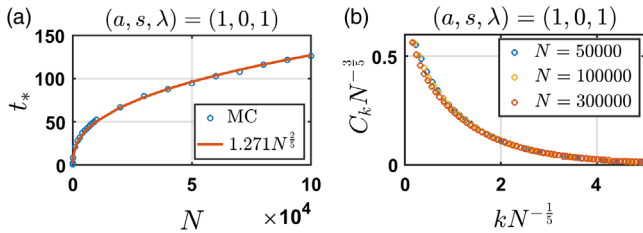


FIG. 4. (a) Crossover time t_* as a function of system size N . Dots are MC results, line is theory, Eq. (28). (b) The final cluster size distribution in the SCS with $(a, s, \lambda) = (1, 0, 1)$ for different N . The data collapse of $C_k(\infty)/N^{3/5}$ on the scaling function $\Phi(\kappa) \sim e^{-b\kappa}$, where $\kappa = k/N^{1/5}$ is observed, $b \approx 0.87$.

$$\langle C_k(\infty) \rangle \sim N^{3/5}e^{-b\kappa}, \quad \kappa = \frac{k}{N^{1/5}}; \quad C(\infty) \sim N^{4/5}, \quad (29)$$

which fairly well agrees with simulations, Fig. 4(b). The nonextensive growth has been detected in a few aggregation-fragmentation processes with standard spontaneous fragmentation [66,67], pure aggregation [68], and pure fragmentation [69]. Neither monomers nor fluctuations play any special role there. In contrast, the SCSs arising in our models are determined by fluctuations.

To summarize, the systems undergoing addition and shattering may fall into a nonextensive state that combines properties of critical and gelling states. As in a critical state, fluctuations play a dominant role; similar to a gelling state, mass is mostly accumulated in huge clusters. In the parameter space, the SCS-related domain is surrounded by standard extensive states, viz equilibrium and jammed states. The transitions between SCS and ES or JS are continuous. Our findings demonstrate that a new approach is needed to describe the SCS, which is beyond the van Kampen expansion. The final cluster distribution is characterized by the exponents α, β, γ :

$$\langle C_k \rangle \simeq N^\gamma \Phi(\kappa), \quad \kappa = kN^{-\alpha}, \quad t_* \sim N^\beta. \quad (30)$$

The total number of clusters scales as N^δ with $\delta = \gamma + \alpha$. Additionally, $\gamma + 2\alpha = 1$, due to mass conservation.

The formation of the SCSs is fluctuation dominated, so the theoretical understanding is challenging even in the simplest cases. We believe that the existence of nonextensive SCSs may have practical implications, for instance, in operating large networks, where SCSs may possibly emerge, similar to the reported JSs [70].

-
- [1] M. V. Smoluchowski, Z. Phys. **17**, 557 (1916).
 - [2] M. V. Smoluchowski, Z. Phys. Chem. **92**, 129 (1917).
 - [3] S. Chandrasekhar, Rev. Mod. Phys. **15**, 1 (1943).
 - [4] P. J. Flory, *Principles of Polymer Chemistry* (Cornell University Press, Ithaca, New York, 1953).
 - [5] P. L. Krapivsky, S. Redner, and E. Ben-Naim, *A Kinetic View of Statistical Physics* (Cambridge University Press, Cambridge, England, 2010).
 - [6] F. Leyvraz, Phys. Rep. **383**, 95 (2003).
 - [7] S. N. Dorogovtsev and J. F. F. Mendes, *Evolution of Networks* (Oxford University Press, Oxford, 2003).
 - [8] G. M. Whitesides and B. Grzybowski, Science **295**, 2418 (2002).
 - [9] K. Ariga, J. P. Hill, M. V. Lee, A. Vinu, R. Charvet, and S. Acharya, Sci. Technol. Adv. Mater. **9**, 014109 (2008).
 - [10] A. Demortire, A. Snezhko, M. V. Sapozhnikov, N. Becker, T. Proslie, and I. S. Aranson, Nat. Commun. **5**, 3117 (2014).
 - [11] C. G. Evans and E. Winfree, Chem. Soc. Rev. **46**, 3808 (2017).

- [12] P. W. K. Rothmund, N. Papadakis, and E. Winfree, *PLoS Biol.* **2**, e424 (2004).
- [13] J. H. Seinfeld and S. N. Pandis, *Atmospheric Chemistry and Physics* (Wiley, New York, 1998).
- [14] H. Pruppacher and J. Klett, *Microphysics of Clouds and Precipitations* (Kluwer, Dordrecht, 1998).
- [15] G. Falkovich, A. Fouxon, and M. G. Stepanov, *Nature (London)* **419**, 151 (2002).
- [16] R. C. Srivastava, *J. Atmos. Sci.* **39**, 1317 (1982).
- [17] L. Esposito, *Planetary Rings* (Cambridge University Press, Cambridge, 2006).
- [18] N. V. Brilliantov, A. S. Bodrova, and P. L. Krapivsky, *J. Stat. Mech.* (2009) P06011.
- [19] C. Güttler, J. Blum, A. Zsom, C. Ormel, and C. P. Dullemond, *Astron. Astrophys.* **513**, A56 (2010).
- [20] M. Lambrechts and A. Johansen, *Astron. Astrophys.* **544**, A32 (2012).
- [21] N. V. Brilliantov, P. L. Krapivsky, A. Bodrova, F. Spahn, H. Hayakawa, V. Stadnichuk, and J. Schmidt, *Proc. Natl. Acad. Sci. U.S.A.* **112**, 9536 (2015).
- [22] C. Singh and M. G. Mazza, *Sci. Rep.* **9**, 9049 (2019).
- [23] J. Blum, *Space Sci. Rev.* **214**, 52 (2018).
- [24] R. Gross, M. Bonani, F. Monada, and M. Dorigo, *IEEE. Trans. Robot.* **22**, 1115 (2006).
- [25] M. Grabisch and A. Rusinowska, *Math. Soc. Sci.* **66**, 316 (2013).
- [26] B. Skyrms and R. Pemantle, *Proc. Natl. Acad. Sci. U.S.A.* **97**, 9340 (2000).
- [27] V. Privman, *Ann. N.Y. Acad. Sci.* **1161**, 508 (2009).
- [28] N. V. Brilliantov and P. L. Krapivsky, *J. Phys. A* **24**, 4789 (1991).
- [29] J. A. Blackman and A. Wielding, *Europhys. Lett.* **16**, 115 (1991).
- [30] J. A. Blackman and A. Marshall, *J. Phys. A* **27**, 725 (1994).
- [31] M. C. Bartelt and J. W. Evans, *Phys. Rev. B* **46**, 12675 (1992).
- [32] H. Kallabis, P. L. Krapivsky, and D. E. Wolf, *Eur. Phys. J. B* **5**, 801 (1998).
- [33] A. Pimpinelli and J. Villain, *Physics of Crystal Growth* (Cambridge University Press, Cambridge, England, 1998).
- [34] M. Zinke-Allmang, *Thin Solid Films* **346**, 1 (1999).
- [35] P. L. Krapivsky, J. F. F. Mendes, and S. Redner, *Eur. Phys. J. B* **4**, 401 (1998).
- [36] P. L. Krapivsky, J. F. F. Mendes, and S. Redner, *Phys. Rev. B* **59**, 15950 (1999).
- [37] J. G. Amar, M. N. Popescu, and F. Family, *Phys. Rev. Lett.* **86**, 3092 (2001).
- [38] V. Gorshkov and V. Privman, *Physica (Amsterdam)* **43E**, 1 (2010).
- [39] I. Sevonkaev, V. Privman, and D. Goia, *J. Chem. Phys.* **138**, 014703 (2013).
- [40] M. Koiwa, *J. Phys. Soc. Jpn.* **37**, 1532 (1974).
- [41] J. Marian and V. V. Bulatov, *J. Nucl. Mater.* **415**, 84 (2011).
- [42] J. M. Ball, J. Carr, and O. Penrose, *Commun. Math. Phys.* **104**, 657 (1986).
- [43] J. R. King and J. A. D. Wattis, *J. Phys. A* **35**, 1357 (2002).
- [44] B. Niethammer, *J. Nonlinear Sci.* **13**, 115 (2003).
- [45] J. A. D. Wattis, *Physica (Amsterdam)* **222D**, 1 (2006).
- [46] J. A. D. Wattis, *J. Phys. A* **42**, 045002 (2009).
- [47] B. Niethammer and R. L. Pego, *J. Stat. Phys.* **95**, 867 (1999).
- [48] M. Herrmann, B. Niethammer, and J. J. L. Velázquez, *J. Differ. Equations* **247**, 2282 (2009).
- [49] P. Laurençot and D. Wrzosek, *J. Stat. Phys.* **104**, 193 (2001).
- [50] J. H. Oort and H. C. van de Hulst, *Bull. Astron. Inst. Netherlands* **10**, 187 (1946), <https://ui.adsabs.harvard.edu/abs/1946BAN....10..187O/abstract>.
- [51] V. Bagland and P. Laurençot, *SIAM J. Math. Anal.* **39**, 345 (2007).
- [52] J. A. D. Wattis, *J. Phys. A* **45**, 425001 (2012).
- [53] P. B. Dubovski, *J. Phys. A* **32**, 781 (1999).
- [54] V. Stadnichuk, A. Bodrova, and N. V. Brilliantov, *Int. J. Mod. Phys. B* **29**, 1550208 (2015).
- [55] S. A. Matveev, P. L. Krapivsky, A. P. Smirnov, E. E. Tyrtshnikov, and N. V. Brilliantov, *Phys. Rev. Lett.* **119**, 260601 (2017).
- [56] P. L. Krapivsky, W. Otieno, and N. V. Brilliantov, *Phys. Rev. E* **96**, 042138 (2017).
- [57] C. Connaughton, A. Dutta, R. Rajesh, N. Siddharth, and O. Zaboronski, *Phys. Rev. E* **97**, 022137 (2018).
- [58] R. Schrapler and J. Blum, *Astrophys. J.* **734**, 108 (2011).
- [59] See Supplemental Material at <http://link.aps.org/supplemental/10.1103/PhysRevLett.127.250602> for the derivation detail, analysis, and results for the related models.
- [60] P. L. Krapivsky and S. Redner, *Phys. Rev. E* **63**, 066123 (2001).
- [61] Y. Zhao, J. Barés, H. Zheng, J. E. S. Socolar, and R. P. Behringer, *Phys. Rev. Lett.* **123**, 158001 (2019).
- [62] Y. Zhang, M. J. Godfrey, and M. A. Moore, *Phys. Rev. E* **102**, 042614 (2020).
- [63] N. V. Brilliantov, W. Otieno, and P. L. Krapivsky (unpublished).
- [64] D. T. Gillespie, *J. Comput. Phys.* **22**, 403 (1976).
- [65] N. van Kampen, *Stochastic Processes in Physics and Chemistry* (North Holland, Amsterdam, 2004).
- [66] E. Ben-Naim and P. L. Krapivsky, *Phys. Rev. E* **77**, 061132 (2008).
- [67] R. S. Hoy and G. H. Fredrickson, *J. Chem. Phys.* **131**, 224902 (2009).
- [68] D. S. Ben-Naim, E. Ben-Naim, and P. L. Krapivsky, *J. Phys. A* **51**, 455002 (2018).
- [69] E. Ben-Naim and P. L. Krapivsky, *Phys. Rev. E* **100**, 032122 (2019).
- [70] M. J. Krawczyk and K. Kulakowski, *Physica (Amsterdam)* **531A**, 121716 (2019).